ACS central science

Research Article

Cite This: ACS Cent. Sci. 2019, 5, 607−618

http://pubs.acs.org/journal/acscii

Mapping the Azolog Space Enables the Optical Control of New Biological Targets

Johannes Morstein,[†,§] Mahendra Awale,[‡,§] Jean-Louis Reymond,*[,‡] and Dirk Trauner*[,†]

[†]Department of Chemistry, New York University, 100 Washington Square East, New York, New York 10003-6699, United States

[‡]Department of Chemistry and Biochemistry, National Center for Competence in Research NCCR TransCure, University of Bern, Freiestrasse 3, 3012 Bern, Switzerland

Supporting Information

ABSTRACT: Photopharmacology relies on molecules that change their biological activity upon irradiation. Many of these are derived from known drugs by replacing their core with an isosteric azobenzene photoswitch (azologization). The question is how many of the known bioactive ligands could be addressed in such a way. Here, we systematically assess the space of molecules amenable to azologization from databases of bioactive molecules (DrugBank, PDB, CHEMBL) and the Cambridge Structural Database. Shape similarity scoring functions (3DAPfp) and analyses of dihedral angles are employed to quantify the structural homology between a bioactive molecule and the *cis* or *trans* isomer of its corresponding azolog ("azoster") and assess which isomer is likely to be active. Our analysis suggests that a very large number of bioactive ligands (>40 000) is amenable to azologization and that many new biological targets could be addressed with photopharmacology. *N*-Aryl benzamides, 1,2-diarylethanes, and benzyl phenyl ethers are particularly suited for this approach, while benzylanilines and sulfonamides appear to be less well-matched. On the basis of our analysis, the majority of azosters are expected to be active in their *trans* form. The broad applicability of our approach is demonstrated with photoswitches that target a nuclear hormone receptor (RAR) and a lipid processing enzyme (LTA_4 hydrolase).

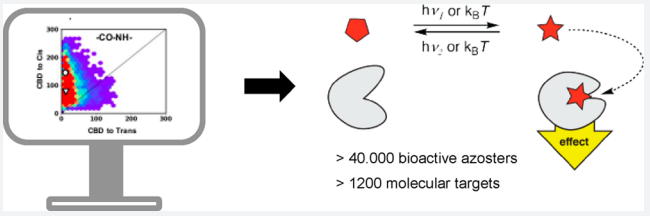

INTRODUCTION

Many biological targets can be modulated by small molecules, which can be modified with a photoswitch to obtain optical control over their function. This approach, termed photopharmacology, has been successfully applied to ion channels, receptors, enzymes, transporters, and elements of the cytoskeleton.[1−3] Many drugs and bioactive molecules possess motifs that resemble azobenzenes; i.e., they feature two arenes separated by a two-atom linker (Figure 1A). Substitution of this linker with a diazene unit (−N═N−) allows for the incorporation of a photoswitch with minimal structural perturbation of the pharmacophore. We call this approach "azologization" and the corresponding isosteric molecules "azosters".[4,5] Ideally, only one isomer of the azolog exhibits the bioactivity of the parent drug, while the other is inactive. A number of stilbenes,[6−12] *N*-aryl benzamides,[13,14] benzyl phenyl ethers,[15,16] and benzyl anilines[17] have been successfully azologed. Other types, such as 1,2-diaryl ethanes, biaryl sulfonamides, *N*-alkyl benzylanilines, could also be amenable to this approach (Figure 1B).

The success of azologization strategies to date raises the question how many bioactive molecules could be put under optical control in such way. To this end, we assessed the suitability of known bioactive ligands for azologization by virtual screening. Candidates from the PDB, ChEMBL, and DrugBank databases were evaluated based on computed structural homology (3DAPfp) and analysis of the dihedral angles of a central four-atom linker (Figure 1C).[18] This analysis leads to the identification of over 40 000 bioactive molecules that should be amenable to azologization, many of which open new target classes for photopharmacology.

RESULTS AND DISCUSSION

Identification of Bioactive Azologs. To confine our search to molecules with known bioactivity, we turned to the databases PDB ligand,[19] DrugBank,[20] and CHEMBL.[21] PDB ligand contains experimentally determined 3D coordinates of molecules in their target-bound conformations, whereas DrugBank and CHEMBL combine 2D data (SMILES strings) with comprehensive drug target information. We also analyzed the Cambridge Structural Database (CSD), the largest source of small molecule single crystal X-ray structures.[22] To identify possible azologable compounds in these databases, we considered all molecules with up to 50 non-hydrogen atoms and selected those containing a pair of aromatic or heteroaromatic ring systems separated by a two-atom linker (e.g., −CH═CH−, $-CH_2-CH_2-$, $-CH_2-NH-$, −CONH−, $-CH_2-O-$, $-CH_2-S-$, $-SO_2-NH-$, and others). In total, we identified more than 180 000 bioactive molecules that meet these criteria (Table 1), the majority of which were *N*-aryl benzamides (>60 000), benzyl phenyl ethers (>23 000), biaryl

Received: November 30, 2018
Published: March 13, 2019

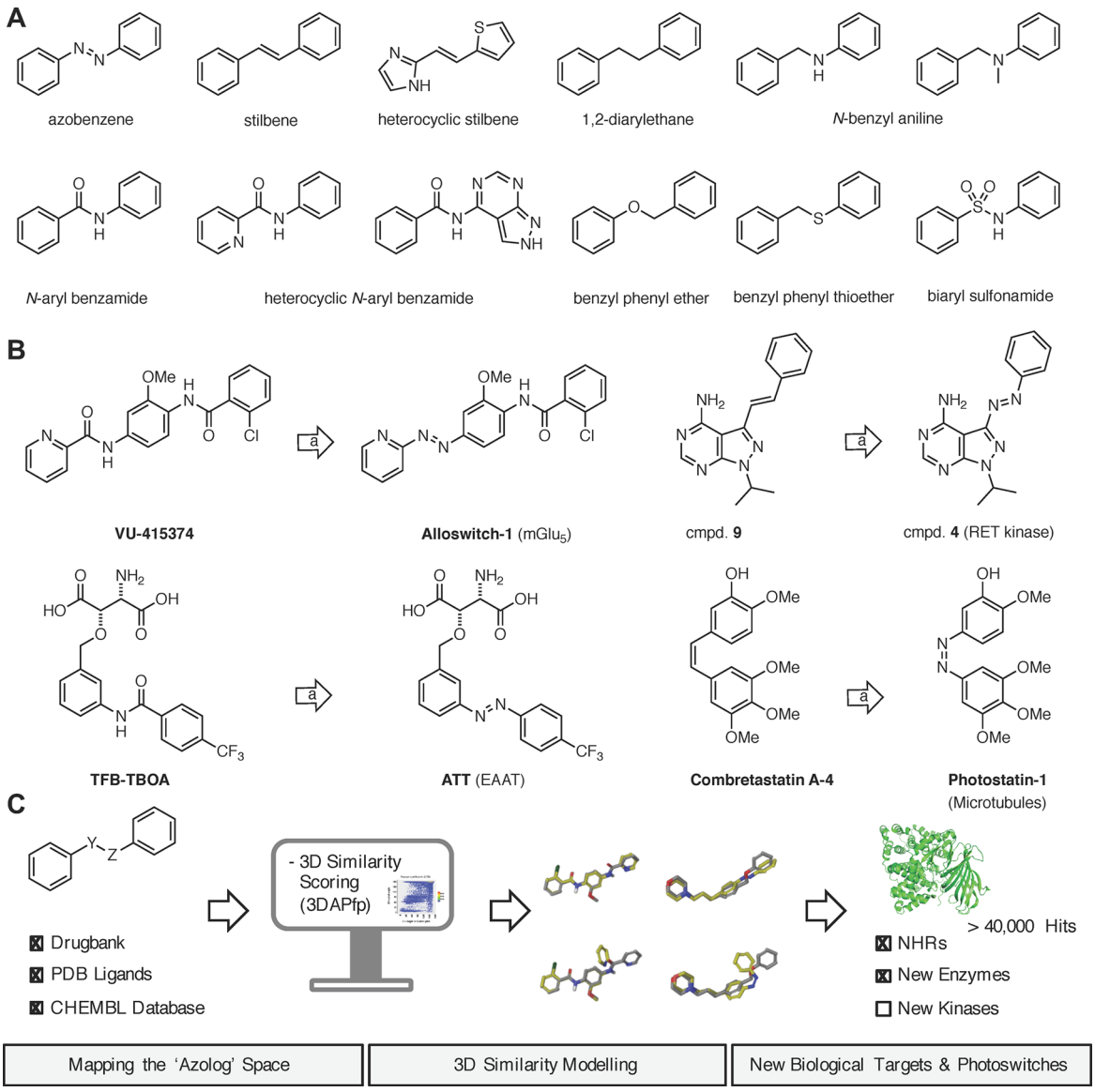

Figure 1. Azologization of bioactive molecules. (A) The structure of azobenzene in its *trans*-form and azosteric motifs found in bioactive molecules. (B) Selected examples of azosters drawn from the literature. (C) Systematic mapping of the photopharmacology space.

Table 1. Overview of Databases

			no. of cmpds as per top five linker types					
database	no. of cmpds	no. of azologable cmpds[a]	−CO−NH−	−NH−CH_2−	−SO_2−NH−	−O−CH_2−	−CH=CH−	no. of linker types
PDB ligand	1,272,030	2,027	603	356	152	236	72	44
CSD	764,008	9,081	1,056	331	654	515	1,303	277
DrugBank	7,133	340	91	54	44	40	16	33
ChEMBL	1,678,393	167,688	59,522	16,263	18,354	22,724	6,856	192

[a]In each database, only unique molecule entries (after counterion removal) containing acyclic linkers were considered. See Experimental Section for details.

sulfonamides (>19 000), and benzyl anilines (>17 000). We also found more than 7000 stilbenes. The 3D coordinates of these molecules were either extracted from the databases (PDB and CSD) or calculated with the 3D structure generator CORINA (Drugbank and ChEMBL).

Analysis of PDB Ligands and CSD Structures. We first turned to the azologable PDB ligands because their target-bound conformations are known and can be directly compared to that of the respective *cis* or *trans* azologs. We also decided to include the experimental structures from the CSD into this analysis which are usually obtained in much higher resolution. To assess which compounds and linker-types are best suited for azologization, we compared the dihedral angles (ω) defined by the C−X−Y−C linkers (Figure 2). Molecules with ω-values close to 180° correspond to *trans*-azologs, while ω-values close to 0° match the angles in *cis*-azologs.

The majority of PDB/CSD structures had dihedral angles close to 180° corresponding to the respective *trans*-azologs.

DOI: 10.1021/acscentsci.8b00881
ACS Cent. Sci. 2019, 5, 607−618

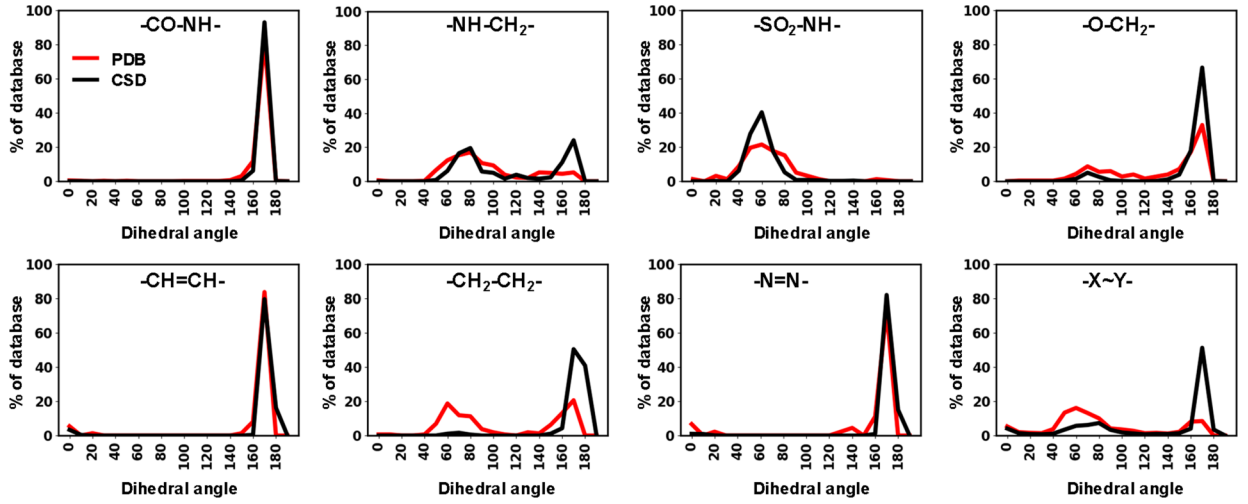

Figure 2. Dihedral angle analysis of PDB and CSD compounds with azologable linkers.

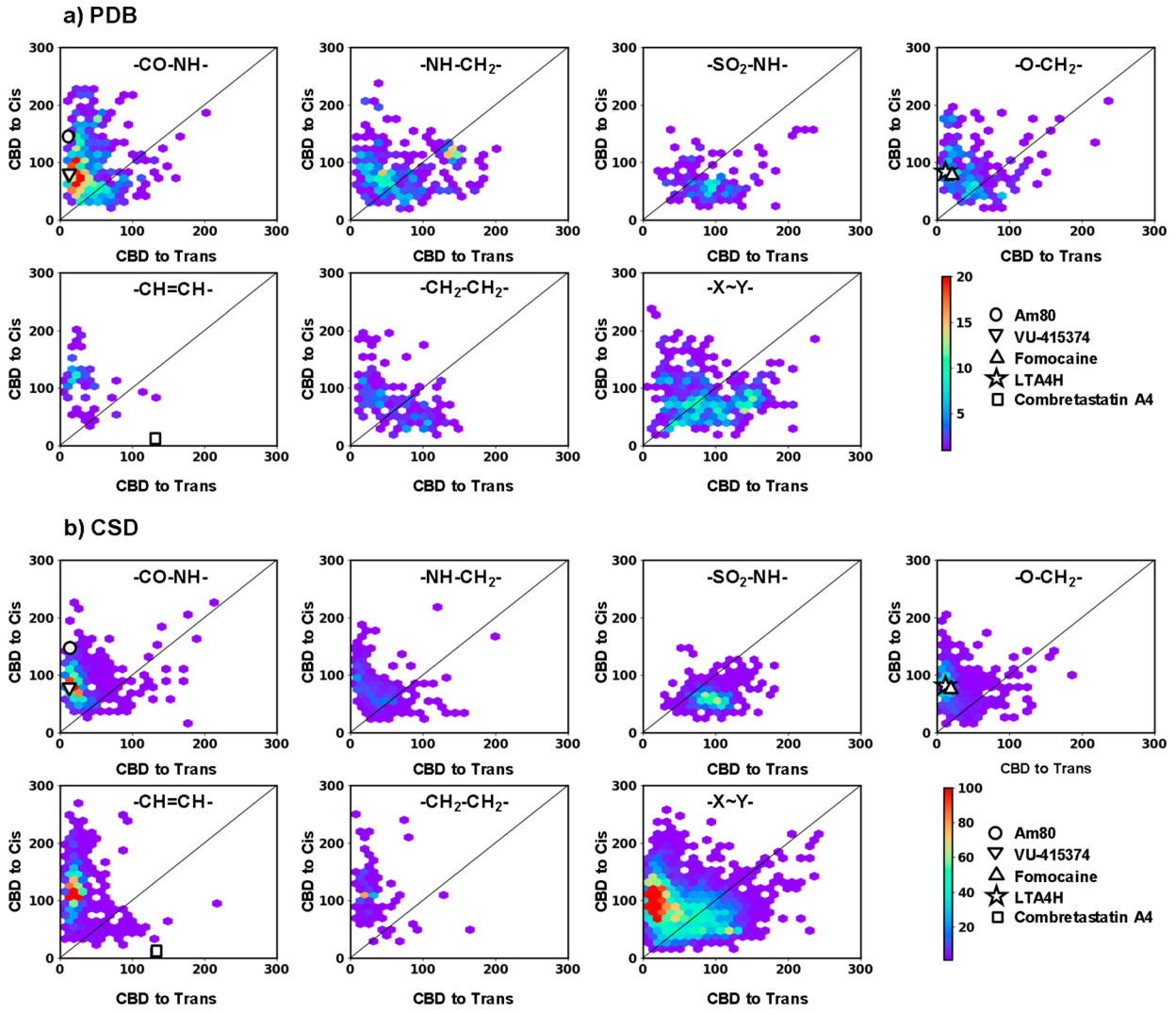

Figure 3. Scatter plots showing the 3D-shape similarities of potential azologable compounds toward their *cis*-azolog (vertical axis) and *trans*-azolog (horizontal axis), for compounds from PDB (a) and CSD (b). 3D Shape similarities are reported as the city block distance (CBD) in the 3DAPfp, with the lowest value indicating highest similarity. Scatter plots are shown for six highly populated linker groups and rest of the groups merged together (−X−Y−). Each of the scatter plots is marked with the structure of respective linker type. Color scale shows the density of molecules. The compounds further investigated in this study are highlighted on the scatter plots.

DOI: 10.1021/acscentsci.8b00881
ACS Cent. Sci. 2019, 5, 607−618

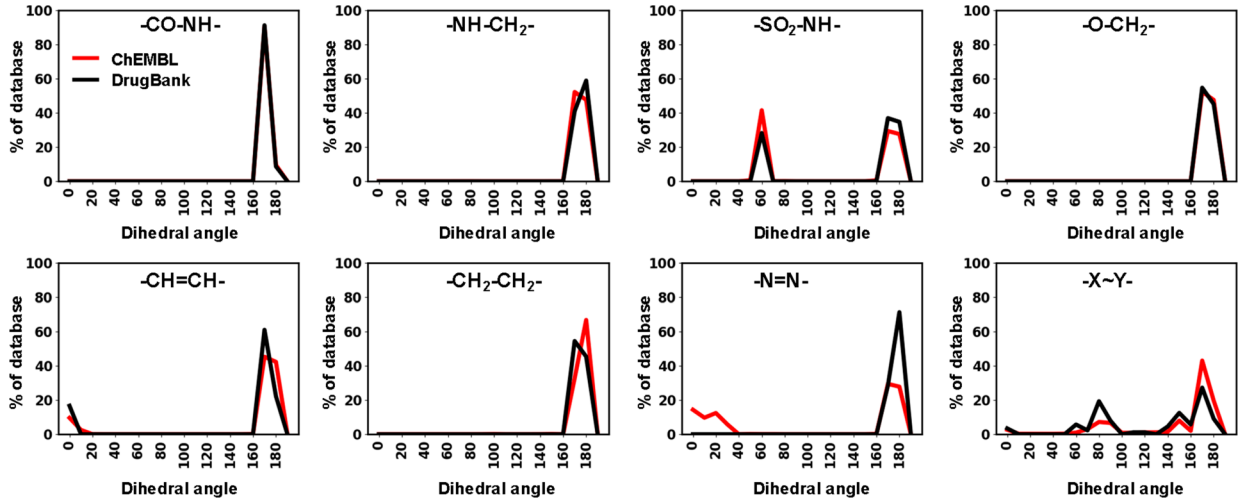

Figure 4. Dihedral angle analysis of ChEMBL and DrugBank compounds with azologable linkers.

For biaryl sulfonamides, benzyl anilines, and benzyl phenyl ethers we observed that a considerable number of representatives had dihedral angle values around 60°. Since this *gauche* confirmation neither fits the geometry of *trans*- nor *cis*-azologs, these compounds are likely less amenable to azologization.

Next, we computationally generated *cis*- and *trans*-azologs for all PDB/CSD structures identified in our screen using the 3D builder CORINA.[23] We compared the shape similarity of the parent compound to the computed *cis*- and *trans*-azologs using the 3D atom pair fingerprint 3DAPfp, which is a 16-dimensional fingerprint counting the number of atom pairs at exponentially increasing distances in a molecule, and which encodes molecular shape.[18] 3D structural homology between parent drug and either azolog isomer was quantified using city block distance (CBD) metric, which is the sum of the absolute differences between the 16 pairs of bit values in the respective 3DAPfp fingerprints, such that a low CBD_{3DAPfp} value indicates a high shape similarity between two molecules. We subsequently analyzed the entire azolog space comparing the CBD values of parent structures with the respective *cis*/*trans* azologs. The results from the analysis were scatter plotted by linker type and database (Figure 3) and are individually discussed for the major compound classes below. In addition, we investigated for each class whether the linker engages in hydrogen bonding, which would be partially or fully lost upon azologization. We arbitrarily selected 30 benzyl anilines, *N*-alkyl benzyl anilines, *N*-aryl benzamides, and biaryl sulfonamides from the PDB ligands and analyzed the crystal structures for potential target engagement (SI Table 1).

Azobenzenes. In addition to the azologable targets analyzed above, PDB and CSD also contained a large number of azobenzenes themselves. Of course, these compounds would be the most straightforward photoswitches to use. In our search for bioactive azobenzenes we found 14 molecules in Drugbank, 45 in PDB, and 1602 in ChEMBL. Similar to the analysis performed above, we analyzed their experimentally determined 3D structures as reported in the PDB and CSD compared the dihedral angles across the C−N═N−C moiety (Figure 2). The majority of the azobenzenes were *trans* isomers with angles close to 180°, whereas a few examples of *cis*-azobenzenes existed that had dihedral angles close to 0° (examples: PDB 2H4B, 2M0Z, and 2CLX). None of the diazene units appear to engage in hydrogen bonding, although azobenzenes are protonated at this site under strongly acidic conditions (the pK_a of methyl orange is 3.4).

Stilbenes. Stilbenes provide the most obvious azologization motif since the dihedral angles of *trans*-stilbenes match those of *trans*-azobenzenes, while *cis*-stilbenes would be expected to give *cis*-active azologs. However, surprisingly few *cis*-stilbenes have been found in our analysis. Combretastatin A-4 is a notable exception (Figure 3).

1,2-Diarylethanes. To the best of our knowledge, 1,2-diarylethanes have not yet been azologed for use in photopharmacology. Their dihedral angle analysis shows that approximately 50% of the PDB ligands bind their biological target with angles closely matching those of *trans*-azobenzenes. Like stilbenes, they cannot engage in hydrogen bonding at the linker region.

***N*-Aryl Benzamides.** The most abundant azologization motifs found are *N*-aryl benzamides. The dihedral angle and 3D structural homology analyses confirm that these molecules should be prime targets for azologization and are expected to give *trans*-active compounds. Their linker amide can function as hydrogen bond donor or acceptor. Azologization could therefore lead to a loss of the bioactivity. However, amide linkers are often employed in medicinal chemistry to connect two fragments with an easily formed bond. Indeed, we found that approximately one-third of carboxamide linkers (11/30) do not engage in hydrogen bonding, increasing the chances that the corresponding azolog has comparable potency to the parent compound.

Benzyl Phenyl Ethers. Benzyl phenyl ethers have been successfully employed on a few occasions. Our study suggests that this linker class is highly amenable to azologization. The majority of benzyl phenyl ethers possesses dihedral angles around 180°, which primes them as potential *trans*-azologs. A few benzyl phenyl ethers have gauche angles making them less suitable for azologization. Only 2 of the 30 benzyl phenyl ethers analyzed showed hydrogen bonding to the linker, which is significantly less compared to *N*-aryl benzamides or benzyl anilines.

***N*-Benzyl Anilines.** While benzyl anilines have been successfully azologed previously, our analysis suggests that only a few of these compounds have suitable dihedral angles. A surprisingly large proportion of these compounds exhibit

DOI: 10.1021/acscentsci.8b00881
ACS Cent. Sci. 2019, 5, 607−618

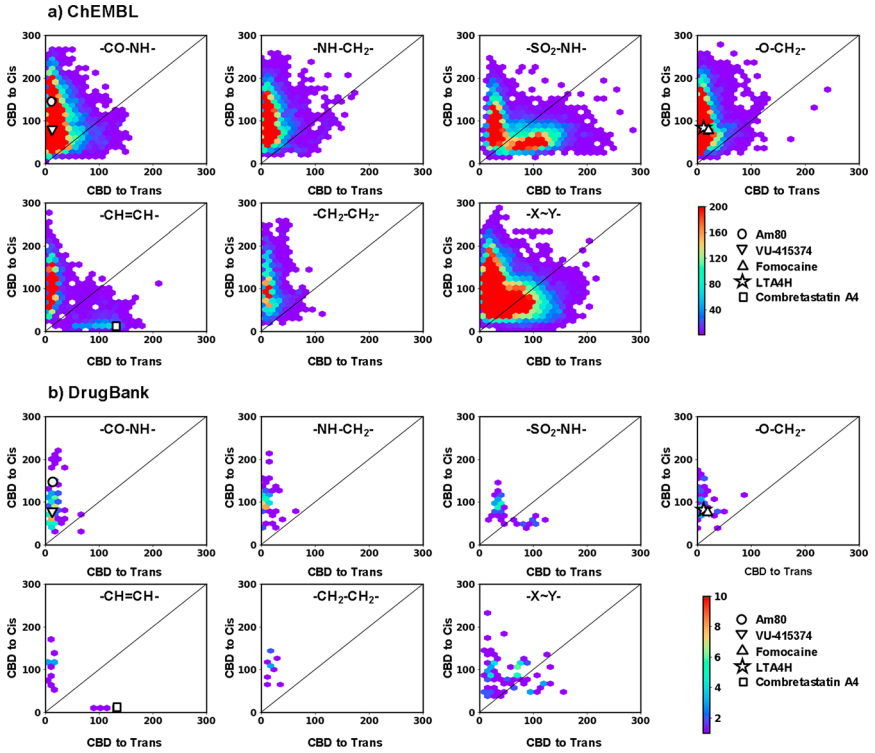

Figure 5. Scatter plots showing the 3D shape similarities of potential azologable compounds toward their *cis*-azolog (vertical axis) and *trans*-azolog (horizontal axis), for compounds from PDB (a) and CSD (b). 3D Shape similarities are reported as the city block distance (CBD) in the 3DAPfp, with lowest value indicating highest similarity. Scatter plots are shown for six highly populated linker groups and rest of the groups merged together (−X−Y−). Each of the scatter plots is marked with the structure of respective linker type. Color scale shows the density of molecules. The compounds further investigated in this study are highlighted on the scatter plots.

gauche-like dihedral angles. Approximately one-third of secondary amine linkers (11/30) and tertiary amine linkers (11/30) show hydrogen bonding in the linker region, which is significantly less than in *N*-aryl benzamides but more than in benzyl phenyl ethers.

Biaryl Sulfonamides. Our analysis suggests that biaryl sulfonamides are generally challenging targets for azologization. They almost exclusively exhibit gauche conformations in their bioactive form and do not show a pronounced tendency for structural overlap with either *trans*- or *cis*-azologs in our 3D structural homology analysis. Roughly one-third of the biaryl sulfonamide analyzed (11/30) also showed hydrogen bonding in the linker region.

Analysis of Drugbank and ChEMBL. Next, we repeated the analysis for Drugbank and ChEMBL using the computationally generated 3D structures (CORINA calculation). With the exception of sulfonamides, all linker types overwhelmingly showed preferred dihedral angles close to 180° (Figure 4).

The scatter plots show similar distributions to that of PDB and CSD compounds, suggesting that the CBD values could indeed be indicative of isomer activity and guide the choice of compounds for azologization (Figure 5). We calibrated this analysis with three known photoswitches, which had previously been developed using an azologization strategy (Figure 6). These include VU-415374, a positive allosteric modulator of metabotropic glutamate receptor type 4, the ion channel blocker fomocaine, and the microtubule inhibitor combretastatin A-4. For VU-415374 and fomocaine, the 3D structure overlay with the respective *trans*-azolog showed more overlap and significantly lower CBD scores compared to that of the *cis*-azolog. For combretastatin A-4 we obtained the reversed result and significantly better overlap between parent drug and *cis*-azolog. These results matched the experimental results and demonstrate that low CBD scores give good predictions about which isomer of an azolog is active.

Azologs and Their Biological Targets. From the analysis above, we selected all molecules from ChEMBL, DrugBank, and PDB having two-atom linkers with experimental or predicted linker dihedral angle falling within the range 0−20° (*cis*-azologization targets) or within the range 160−180° (*trans*-azologization targets; Table 2).

We analyzed these hits according to biological targets. In total, more than 1200 biological targets in the CHEMBL database could be amenable to azologization. Multiple hits were found for most, which increases the chances to find a useful photopharmaceutical. Strikingly, only a small fraction of these biological targets has been previously addressed by photopharmacology. For example, relatively few enzymes found were put under photocontrol. Kinases present the largest class of biological targets that were identified in our screen (Figure 7). While some efforts in optogenetics have been geared toward the optical control of kinases, only a few studies in photopharmacology have addressed them. Other target classes that could benefit from the spatiotemporal resolution of photopharmacology include transcription factors, GPCRs, ion channels, and transporters.

Optical Control of RARα Receptor. To demonstrate the usefulness of our analysis, we synthesized and evaluated a number of hits. To this end, we chose molecules that are easily synthetically accessible and could modulate biological targets that have not been previously addressed with photopharmacology.

DOI: 10.1021/acscentsci.8b00881
ACS Cent. Sci. 2019, 5, 607−618

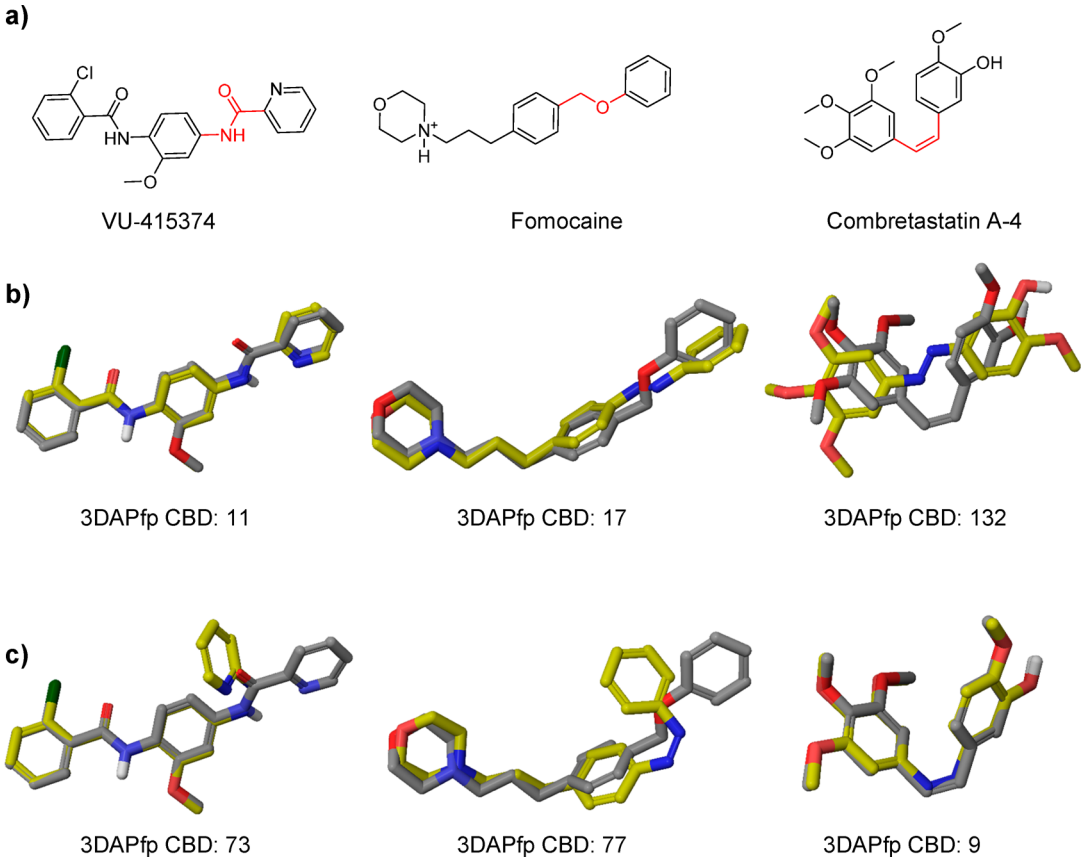

Figure 6. (a) Structures of previously reported azologable compounds. The two atom linkers which were replaced by the diazo group are highlighted in red. (b) 3D-overlays of parent azologable compounds (gray) with corresponding *trans*-azologs (yellow). (c) 3D-overlays of parent azologable compounds (gray) with corresponding *cis*-azologs (yellow).

Table 2. Azologable Compounds

		no. of cmpds. as per top five linker types				
database	no. of azologable cmpds	−CO−NH−	−NH−CH_2−	−SO_2−NH−	−O−CH_2−	−CH═CH−
PDB Ligand	949	577	37	5	117	70
DrugBank	281	91	54	32	40	16
ChEMBL	40,719	16,097	4,746	3,915	7,785	1,186

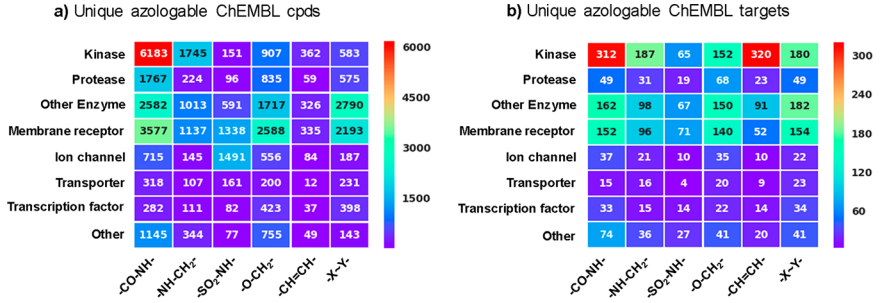

Figure 7. Heatmaps showing (a) number of unique ChEMBL compounds and (b) number of unique ChEMBL targets as a function of linker type and protein target family. Only azologable compounds within the correct predicted dihedral angle windows having IC_{50} and EC_{50} values of <10 μM (~41 K compounds) were considered for this analysis.

Nuclear hormone receptors (NHRs) are hormone targeted transcription factors which bind to DNA and regulate various biological processes.[24,25] Apart from the modulation of transcription levels on a relatively slow time scale, several NHRs are known to mediate rapid nongenomic effects which are thought to occur through protein−protein interactions.[26] Nongenomic functions of NHRs include the regulation of kinases, phosphatase, and ion channels.[27] Optical control of NHRs could enable the dissection between genomic and nongenomic mechanisms with the resolution of single cells in complex cellular networks.

Our computational screen for azologization motifs led to the identification of several hits for a number of nuclear hormone receptors, including retinoic X receptor, retinoic acid receptor,

DOI: 10.1021/acscentsci.8b00881
ACS Cent. Sci. 2019, 5, 607−618

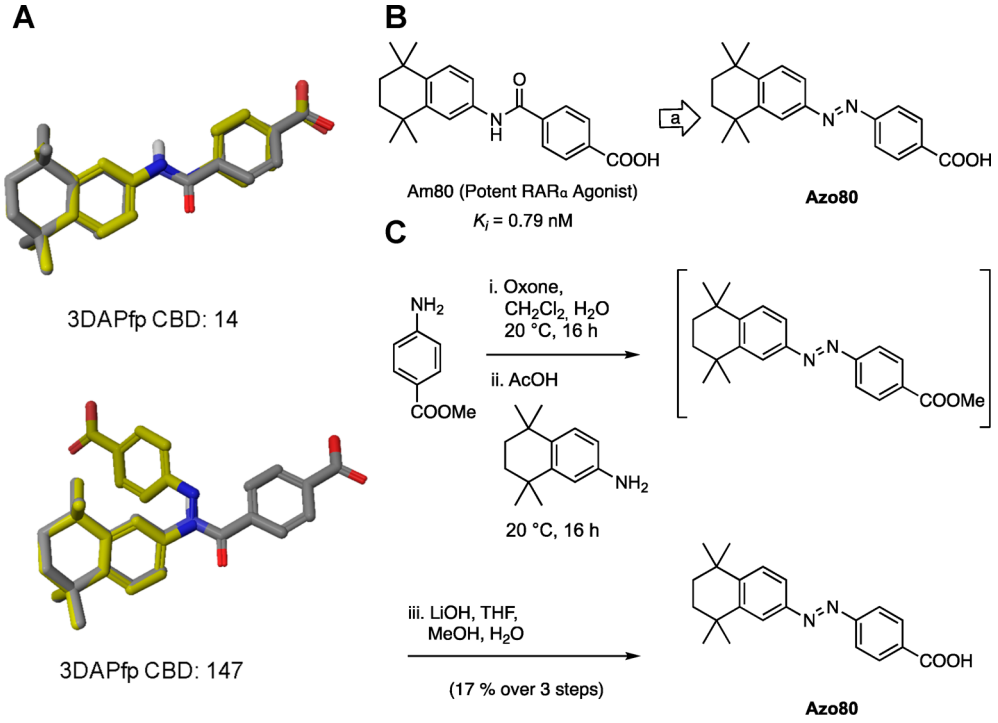

Figure 8. Computational prediction, design, and synthesis of **Azo80**. (A) 3D overlays of parent azologable compounds (gray) with corresponding *cis*- and *trans*- azologs (yellow) and 3DAPfp scores of 3D shape similarity comparison. (B) Design of **Azo80** based on the azologization of the *N*-aryl benzamides Am80. (C) Chemical synthesis of **Azo80**.

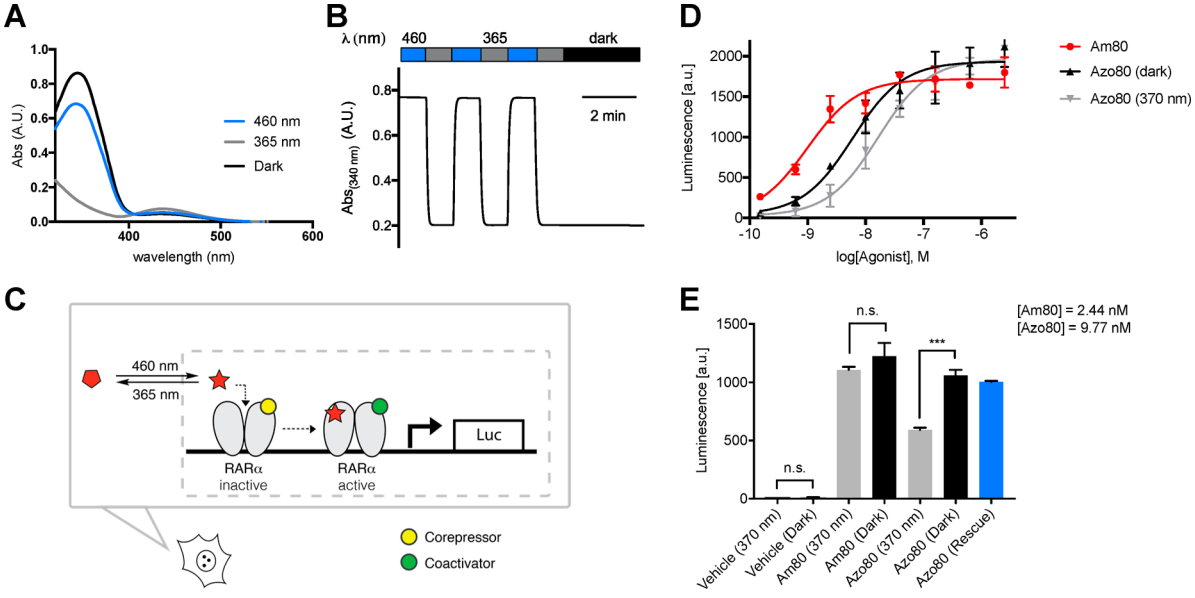

Figure 9. Photophysical and biological evaluation of **Azo80**. (A) The UV−vis spectrum of **Azo80** in the dark-adapted (black, *trans*), 365 nm adapted (gray, *cis*), and 460 nm adapted (blue, *trans*) photostationary states. (B) Reversible cycling between isomers with alternating illumination at 365/460 nm. (C) Schematic depiction of RARα activation with a small molecule photoswitch leading to corepressor/coactivator exchange and transcription of target genes (here: luciferase−luc). (D) Dose responses of Am80, *cis*-**Azo80**, and *trans*-**Azo80** in a luminescent reporter cell line after 22 h. Samples were run in duplicates and in two independent experiments. Error bars represent mean ± SD (E) Control and rescue (reversibility) experiments. Samples were run in triplicates. Error bars represent SEM *** $p < 0.001$, n.s., not significant, student's *t*-test.

thyroid hormone receptor, peroxisome proliferator-activated receptor, liver X receptor, and estrogen receptor. We decided to synthesize the azolog of one of these compounds targeting retinoic acid receptor α (RARα). The potent RARα agonist Am80 is commercially available and widely used in biological research. At the same time our screen suggests that Am80 is an ideal target for azologization (3DAPfp CBD *trans*: 14; 3DAPfp *cis*: 147; Figure 8 A). Interestingly, the azolog of Am80 was already synthesized in 1989 and evaluated in SAR studies (CHEMBL 13150).[28] However, its potential for optical control has never been evaluated, and the compound was exclusively tested in its nonirradiated form. We resynthesized the azolog of Am80, termed **Azo80** (Figure 8B), using Baeyer-Mills conditions with subsequent ester hydrolysis (Figure 8C).

DOI: 10.1021/acscentsci.8b00881
ACS Cent. Sci. 2019, 5, 607−618

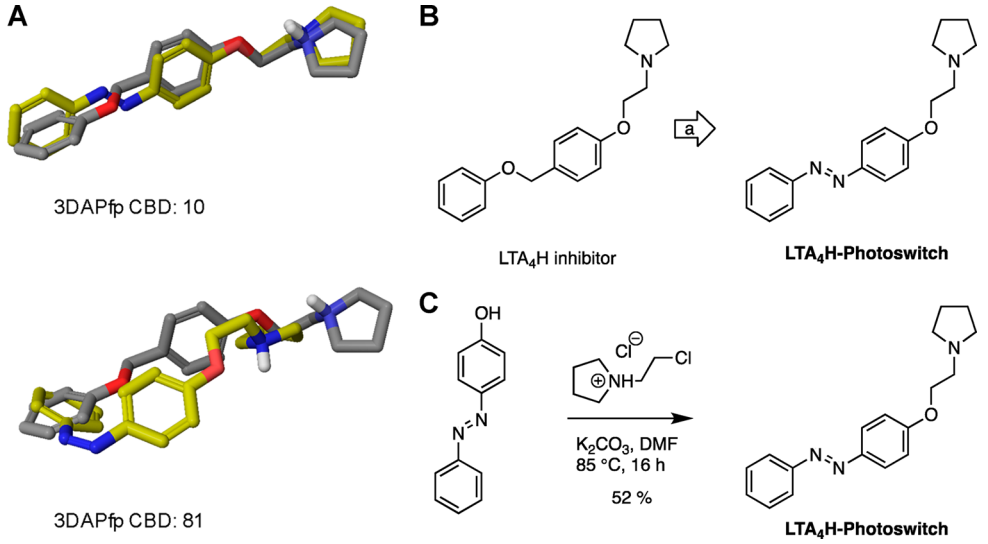

Figure 10. Synthesis and isomerization of **LTA$_4$h-Photoswitch**. (A) 3D-overlays of parent azologable compounds (gray) with corresponding *cis*- and *trans*- azologs (yellow) and 3DAPfp scores of 3D shape similarity comparison. (B) Design of **LTA$_4$h-Photoswitch** based on the azologization of a benzyl phenyl ethers. (C) Chemical synthesis of **LTA$_4$h-Photoswitch**.

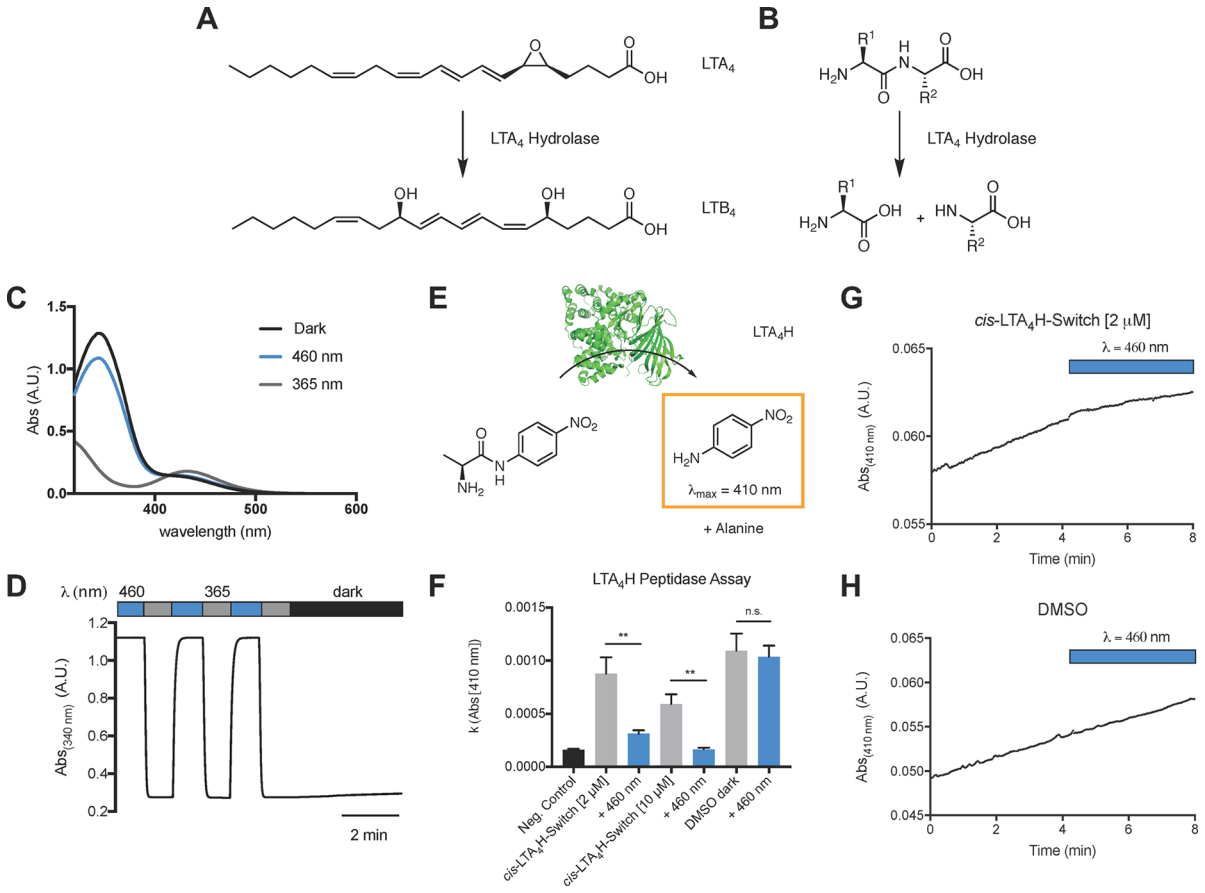

Figure 11. Photophysical evaluation and LTA$_4$-hydrolase peptidase assay with **LTA$_4$H-Photoswitch**. (A, B) Enzymatic reactions catalyzed by LTA$_4$-hydrolase. (C) The UV−vis spectrum of **LTA$_4$H-Photoswitch** in the dark-adapted (black, *trans*), 365 nm adapted (gray, *cis*), and 460 nm adapted (blue, *trans*) photostationary states. (D) Reversible cycling between isomers with alternating illumination at 365/460 nm. (E) Schematic depiction of L-alanine 4-nitroanilide cleavage by LTA$_4$H (PDB: 2VJ8[34]). (F) LTA$_4$H peptidase assay with LTA$_4$ h (1.1 μg) and L-alanine 4-nitroanilide (1 mM) in the presence and absence of *cis*-**LTA$_4$H-Photoswitch** at different concentrations. Samples were irradiated with 460 nm light after 4 min to yield *trans*-**LTA$_4$H-Photoswitch**. The slope of 4-nitroaniline absorption (λ = 410 nm) was plotted. (G, H) Representative traces of 4-nitroaniline absorption (λ = 410 nm) before and after application of 460 nm light. Samples were run in triplicates. Error bars represent SEM ** p < 0.01, n.s., not significant, student's t-test.

DOI: 10.1021/acscentsci.8b00881
ACS Cent. Sci. 2019, 5, 607−618

The photophysical properties of **Azo80** are similar to those of a classical nonsubstituted azobenzene. **Azo80** can be efficiently switched between *cis*/*trans* using 365/460 nm light and is bistable (Figure 9A,B). To test **Azo80** for the ability to photocontrol RARα, we used a reporter gene assay in which the activation of RARα induces transcription of luciferase (Figure 9C). Upon addition of luciferase substrate after 24 h incubation, a luminescent signal proportional to luciferase transcription and RARα activation was quantified. We were pleased to find that the EC_{50} of *cis*-**Azo80** (1.6×10^{-8} M) is significantly lower than that of *trans*-**Azo80** (6.0×10^{-9} M) (Figure 9D). In a subsequent control experiment (Figure 9E), we demonstrated that light does not mediate or alter transcription levels in the absence of **Azo80**, while reversible optical control is achieved with **Azo80**. To demonstrate reversibility, **Azo80** was added to cells as 365 nm-adapted *cis*-**Azo80** and after 5 min the cells were illuminated with 460 nm light for 2 min to reactivate **Azo80**. Similar levels of transcription were observed in this rescue experiment compared to the experiment with dark-adapted *trans*-**Azo80**. The *trans*-activity of **Azo80** is coherent with the computational prediction, which suggested better 3D homology of Am80 with its *trans*-azolog.

Optical Control of Leuktriene-A4 Hydrolase. Lipid photopharmacology is a rapidly growing field, and photoswitchable lipids have enabled the control of a wide range of biological pathways.[29−31] In this context, the optical modulation of lipid metabolic networks could provide important insights. Our computational screen identified a number of small molecules that target various lipid metabolizing enzymes, including fatty acid amide hydrolases, lipoxygenases, phospholipases, leukotriene hydrolases, lipid kinases, and phosphorylases. Many of these enzymes could be interesting targets for photopharmacology. We decided to synthesize and test a photoswitchable inhibitor of the enzyme Leukotriene A4 hydrolase (LTA_4H). LTA_4H is a dual enzyme that functions both as a hydrolase and as aminopeptidase (Figure 11).[32] It catalyzes the conversion of LTA_4 to LTB_4 and the degradation of chemoattractant tripeptide molecules. Multiple inhibitors for LTA_4H have been in development as anti-inflammatory drugs.[33] The CHEMBL database contained several benzyl phenyl ether based LTA_4H inhibitors, and we chose a relatively potent candidate of this compound family with straightforward synthesis for azologization (Figure 10). The CBD values suggest that this inhibitor exhibits more structural homology with its *trans*-azolog (3DAPfp CBD *trans*: 10; 3DAPfp *cis*: 81; Figure 10 A). **LTA_4h-Photoswitch** was synthesized from 4-phenylazophenol through Williamson ether synthesis (Figure 10C).

We used a colorimetric LTA_4H peptidase assay to evaluate the potential of **LTA_4H-Photoswitch** for the optical control of LTA_4H aminopeptidase activity using L-alanine 4-nitroanilide which is converted to the strongly absorbing 4-nitroaniline (λ = 410). This assay is most commonly used to screen for LTA_4H inhibitors. In good agreement with the computational prediction, *trans*-**LTA_4H-Photoswitch** was a more potent inhibitor of LTA_4H peptidase than the *cis*-isomer (Figure 11).

Azo80 and **LTA_4H-Photoswitch** are two new photoswitches obtained through the azologization of a *N*-aryl benzamide and a benzyl phenyl ether which were identified through the mapping of the photopharmacological azolog space in CHEMBL. These examples demonstrate the utility of the database for the development of bioactive photoswitches for the modulation of new photopharmacological targets from two different azologization motifs.

Concluding Remarks. Our study sheds light on the scope and limitations of azologization in photopharmacology. The azolog space was found to be surprisingly large, comprising more than 40 000 bioactive molecules, which modulate more than 1200 biological targets. Relatively few of those have been put under optical control to date. The identification of functional azologs for two completely different new targets classes (LTA_4H and RARα) illustrates the usefulness of our systematic approach.

3DAPfp shape similarity scores and analysis of dihedral angles gave good predictions of the active isomer for the examples explored and for the newly developed photoswitches reported. These scores could be used to predict which isomer is bioactive. Additional insights for the design and prediction can often be drawn from crystal structures and structure activity relationship studies.

Our results suggest that stilbenes, 1,2-diarylethanes, *N*-aryl benzamides, and benzyl phenyl ethers are excellent candidates for azologization. Benzylanilines and especially sulfonamides appear to be less suited for this approach. The analysis of both dihedral angles and shape similarity indicates that the vast majority of azologs are likely to be more bioactive in their *trans*-form. Usually *cis*-active photoswitches are more desirable as they are inactive in the dark-adapted state and can be activated with light. However, *trans*-active compounds can still be highly useful (e.g., as tonic ion channel blockers) and bistable photoswitches that can be easily kept in the inactive *cis*-state. In addition, *cis*-stable azobenzene photoswitches are emerging that could be adapted to photopharmacology.[35]

The large number of potential molecular targets (>1200) that should be addressable with photopharmacology suggests that this approach to optical control is very versatile. It should be noted, however, that methods other than azologization further increase the reach of photopharmacology. Many photoswitches were designed through extension of the core with azobenzenes instead of replacement ("azo-extension" approach). An *n*-alkyl chain has been replaced with an azobenzene in the optical control of glycerophospho- and sphingolipids. In addition, photoswitches have been successfully installed in the backbone or side chain of biopolymers, such as nucleic acids and peptides. While "azologization" is the most straightforward design strategy, all existing strategies complement each other to provide an exceptionally versatile photopharmacological toolbox.

EXPERIMENTAL SECTION

Processing of Database and Azologs Generation. DrugBank (version 5, https://www.drugbank.ca/), PDB ligands (http://ligand-expo.rcsb.org/ld-download.html), and ChEMBL (version 22, https://www.ebi.ac.uk/chembl/) databases were downloaded in SDF format from the respective database Web site in year 2017. CSD was copied from a licensed CD to Dr. Jürg Hauser, University of Bern. Molecules were processed using an in-house developed Java program utilizing the JChem chemistry library from ChemAxon Pvt. Ltd. (https://www.chemaxon.com/). Counter ions were removed, valence errors were checked, and molecules were ionized at pH 7.4. Molecules containing ≥6 and ≤50 heavy atoms, ≤4 stereocenters, 1 Ar-(two atom linker)-Ar, and no Ar-(diazo linker)-Ar were retained in the database. "Ar" stands for aromatic carbon. The two atoms in linker are acyclic atoms

DOI: 10.1021/acscentsci.8b00881
ACS Cent. Sci. 2019, 5, 607−618

and may or may not be substituted. For each database, duplicate molecules were removed based on unique smiles comparisons. The resulting molecules in these processed databases are considered as potential azologable compounds. Afterward for each of the azologable molecules, Ar-(two atom linker)-Ar was replaced by Ar-(diazo linker)-Ar, and corresponding *trans*- and *cis*-azologs were generated. It should be noted that, whenever the difference in number of atoms between parent azologable molecules and corresponding azologs were more than six atoms, the corresponding molecules were not considered in the study. This was because some of the two atom linkers in parent molecules were substituted by large groups.

Similarity Calculation. For each drug and its two isomeric azolog, we generated the lowest energy 3D conformer using the CORINA program available from Molecular Networks Pvt. Ltd. For the parent azologable compounds in PDB and CSD databases experimental 3D coordinates were used. To compare molecules, we used an in-house developed 3D atom pair fingerprint as a measure of overall shape similarity.[36] For each parent drug and its corresponding *cis* and *trans* azolog 3D atom pair fingerprints were computed, and similarities between them were quantified using city block distance metric.

Chemical Synthesis. All reagents and solvents were purchased from commercial sources (Sigma-Aldrich, TCI Europe N.V., Strem Chemicals, etc.) and were used without further purification. Solvents were obtained from Fisher Scientific. Reactions were monitored by TLC on precoated, Merck Silica gel 60 F_{254} glass backed plates, and the chromatograms were first visualized by UV irradiation at λ = 254 nm. Flash silica gel chromatography was performed using silica gel (SiO_2, particle size 40−63 μm) purchased from SiliCycle. NMR spectra were measured on a BRUKER Avance III HD 400 (equipped with a CryoProbe). Multiplicities in the following experimental procedures are abbreviated as follows: s = singlet, d = doublet, t = triplet, q = quartet, m = multiplet. Proton chemical shifts are expressed in parts per million (ppm, δ scale) and are referenced to the residual protium in the NMR solvent ($CDCl_3$ = 7.26; MeOD: δ = 3.31). Carbon chemical shifts are expressed in ppm (δ scale) and are referenced to the carbon resonance of the NMR solvent (($CDCl_3$: δ = 77.16; MeOD: δ = 49.00). NOTE: Due to the *trans*/*cis* isomerization of some compounds containing an azobenzene functionality, more signals were observed in the ^{1}H and ^{13}C spectra than would be expected for the pure *trans*-isomer. Only signals for the major *trans*-isomer are reported.

Photophysical Evaluation. UV−vis spectra were recorded using a Varian Cary 50 Bio UV−visible spectrophotometer with Hellma SUPRASIL precision cuvettes (10 mm light path). Switching was achieved using 365 or 460 nm LED light sources. The LEDs were pointed directly into the top of the sample cuvette. An initial spectrum was recorded (dark-adapted state, black) and then again following illumination at λ = 365 nm for 30 s (*cis*-adapted state, gray). A third spectrum was recorded after irradiation at λ = 470 nm for 30 s (*trans*-adapted state, blue).

Azo80. A solution of Oxone (378 mg, 0.615 mmol, 2.5 equiv) in water (2 mL) was added to a solution of 4-aminobenzoate (37.2 mg, 0.246 mmol, 1.0 equiv) in CH_2Cl_2 (2 mL), and the biphasic mixture was stirred for 16 h at rt. The organic layer was washed with 1 M HCl, sat. $NaHCO_3$, water, dried over sodium sulfate, filtered, and concentrated *in vacuo*. 5,6,7,8-Tetrahydro-5,5,8,8-tetramethyl-2-naphthylamine (50.0 mg, 0.246 mmol, 1.0 equiv) and acetic acid (2.0 mL) were added and stirred for 24 h at rt. Acetic acid was removed *in vacuo*, and the residue was dissolved in CH_2Cl_2, washed with sat. $NaHCO_3$, water, dried over sodium sulfate, filtered, and concentrated *in vacuo*. The residue was dissolved in THF/MeOH (2 mL/2 mL), treated with 1 M LiOH (1 mL), stirred for 2 h at rt, and acidified with 2 M HCl. It was diluted with EtOAc, washed with water, dried over sodium sulfate, filtered, and concentrated *in vacuo*. Purification by flash column chromatography (CH2Cl2 + 1% AcOH) afforded **Azo80** (13.8 mg, 0.041 mmol, 17%) as an orange solid. A small amount of methanol was added to obtain a more concentrated solution for the ^{13}C NMR measurement. ^{1}H NMR (400 MHz, $CDCl_3$) δ 8.32−8.04 (m, 3H), 7.89 (d, J = 1.8 Hz, 1H), 7.86 (d, J = 7.7 Hz, 2H), 7.63 (dd, J = 8.5, 1.9 Hz, 1H), 7.40 (d, J = 8.5 Hz, 1H), 1.69 (s, 4H), 1.33 (s, 6H), 1.28 (s, 6H). ^{13}C NMR (100 MHz, $CDCl_3$) δ 155.5, 150.7, 149.5, 146.2, 131.0, 127.6, 123.6, 123.4, 122.4, 118.5, 35.0, 34.9, 34.8, 34.6, 31.8, 31.7. HRMS: m/z calcd. for $C_{21}H_{23}N_2O_2^-$ ([M + H]$^-$): 335.1765, found: 335.1758.

LTA$_4$H-Photoswitch. A solution of 1-(2-chloroethyl)-pyrrolidine·HCl (51.4 mg, 0.30 mmol, 1.2 equiv), 4-phenylazophenol (50.0 mg, 0.25 mmol, 1.0 equiv), and K_2CO_3 (104 mg, 0.76 mmol, 3.0 equiv) in DMF (3 mL) was stirred at 85 °C for 16 h. The solution was cooled, water was added, and extracted with EtOAc. The combined organic phase was dried over Na_2SO_4, and concentrated *in vacuo*. Purification by flash column chromatography with CH_2Cl_2 → 10% MeOH in CH_2Cl_2 yielded **LTA$_4$H-Photoswitch** (38.6 mg, 0.13 mmol, 52%) as an orange liquid. ^{1}H NMR (400 MHz, MeOD): δ 7.93−7.81 (m, 4H), 7.55−7.39 (m, 3H), 7.11−7.04 (m, 2H), 4.19 (t, J = 5.6 Hz, 2H), 2.94 (t, J = 5.6 Hz, 2H), 2.68 (t, J = 6.6 Hz, 4H), 1.86−1.78 (m, 4H). ^{13}C NMR (100 MHz, MeOD): δ 162.8, 154.0, 148.3, 131.6, 130.2, 125.8, 123.5, 115.9, 67.9, 55.5, 24.2. HRMS: m/z calcd. for $C_{18}H_{22}N_3O$ ([M + H]$^+$): 296.1757, found: 296.1757.

RARα Reporter Gene Assay. A cell-based human RARα (NR1B1) driven luciferase reporter assay from INDIGO Bioscience (State College, PA) was adapted and used for the biological evaluation of **Azo80**. In brief, a 10 mM stock solution of Am80 or **Azo80** was diluted with the provided cell screening medium to a final concentration of 2.5 μM. A 4-fold dilution series was prepared using this initial concentration and cell screening medium. The dilutions were added to reporter cells in white-bottom 96-well plates. For *trans*-**Azo80**, dilutions were added in the dark and cells were incubated for 22 h in the dark. For *cis*-**Azo80**, dilutions were irradiated at 365 nm for 3 min, and cells were incubated for 22 h in the presence of a 370 nm LED Cell Disco with light pulses for 75 ms/15 s. To minimize variations in the dilutions, the same dilutions were used for both experiments before and after irradiation. For the rescue experiment, **Azo80** was added to cells as 365 nm adapted *cis*-**Azo80** and cells were illuminated after 5 min with 460 nm light for 2 min to reactivate **Azo80**. After 22 h medium was ejected, and the supplied luciferase detection reagents were added and quantified using a BMG Labtech FLUOstar Omega plate reader.

LTA$_4$H-Peptidase Assay. Recombinant LTA$_4$H was purchased from Cayman Chemicals and stored at −80 °C. LTA$_4$H (1.1 μg) was incubated with L-alanine-*p*-nitroanilide (1 mM), in 50 mM HEPES (pH = 7.5), 100 mM KCl, 1 mg/mL BSA, 1% DMSO in the presence and absence of **LTA$_4$H-Photoswitch**. **LTA$_4$H-Photoswitch** was illuminated with 365

DOI: 10.1021/acscentsci.8b00881
ACS Cent. Sci. 2019, 5, 607−618

nm light for 3 min before addition of L-alanine-*p*-nitroanilide, and the reaction was initiated with LTA_4H added last. The absorption at 410 nm was recorded for 4 min. After 4 min a 460 nm LED was used to illuminate the sample in the cuvette, and the absorption was recorded for 4 min under constant illumination.

Safety Statement. No unexpected or unusually high safety hazards were encountered in this line of research.

■ ASSOCIATED CONTENT

Supporting Information

The Supporting Information is available free of charge on the ACS Publications website at DOI: 10.1021/acscentsci.8b00881.

Analysis of linker−protein contacts, analysis of correlation between similarity scatter plot and dihedral angle, compound characterization by NMR and HRMS (PDF)

■ AUTHOR INFORMATION

Corresponding Authors

*(J.L.R.) E-mail: jean-louis.reymond@dcb.unibe.ch.
*(D.T.) E-mail: dirktrauner@nyu.edu.

ORCID

Johannes Morstein: 0000-0002-6940-288X
Jean-Louis Reymond: 0000-0003-2724-2942
Dirk Trauner: 0000-0002-6782-6056

Author Contributions

§J.M. and M.A. contributed equally.

Notes

The authors declare no competing financial interest.

■ ACKNOWLEDGMENTS

We thank New York University for financial support. NMR spectra were acquired using the TCI cryoprobe supported by the NIH (OD016343). This work was supported financially by the Swiss National Science Foundation, NCCR TransCure. J.M. thanks the German Academic Scholarship Foundation for a Ph.D. fellowship and New York University for a MacCracken Ph.D. fellowship. Dr. Bryan Matsuura, Christopher Arp, Martin Reynders, Konstantin Hinnah, Dr. Andrej Shemet, and Dr. Christian Fischer are acknowledged for insightful discussion and critical review of the manuscript.

■ REFERENCES

(1) Hüll, K.; Morstein, J.; Trauner, D. *In Vivo* Photopharmacology. *Chem. Rev.* **2018**, *118*, 10710−10747.
(2) Beharry, A. A.; Woolley, G. A. Azobenzene Photoswitches for Biomolecules. *Chem. Soc. Rev.* **2011**, *40*, 4422−4437.
(3) Velema, W. A.; Szymanski, W.; Feringa, B. L. Photopharmacology: Beyond Proof of Principle. *J. Am. Chem. Soc.* **2014**, *136*, 2178−2191.
(4) Broichhagen, J.; Frank, J. A.; Trauner, D. A Roadmap to Success in Photopharmacology. *Acc. Chem. Res.* **2015**, *48*, 1947−1960.
(5) Schoenberger, M.; Damijonaitis, A.; Zhang, Z.; Nagel, D.; Trauner, D. Development of a New Photochromic Ion Channel Blocker via Azologization of Fomocaine. *ACS Chem. Neurosci.* **2014**, *5*, 514−518.
(6) Borowiak, M.; Nahaboo, W.; Reynders, M.; Nekolla, K.; Jalinot, P.; Hasserodt, J.; Rehberg, M.; Delattre, M.; Zahler, S.; Vollmar, A.; et al. Photoswitchable Inhibitors of Microtubule Dynamics Optically Control Mitosis and Cell Death. *Cell* **2015**, *162*, 403−411.
(7) Engdahl, A. J.; Torres, E. A.; Lock, S. E.; Engdahl, T. B.; Mertz, P. S.; Streu, C. N. Synthesis, Characterization, and Bioactivity of the Photoisomerizable Tubulin Polymerization Inhibitor Azo-Combretastatin A4. *Org. Lett.* **2015**, *17*, 4546−4549.
(8) Sheldon, E.; Dcona, M. M.; Lyons, C. E.; Hackett, J. C.; Hartman, M. C. T. Photoswitchable Anticancer Activity via Trans − Cis Isomerization of a Combretastatin A-4 Analog. *Org. Biomol. Chem.* **2016**, *14*, 40−49.
(9) Damijonaitis, A.; Broichhagen, J.; Urushima, T.; Hull, K.; Nagpal, J.; Laprell, L.; Schonberger, M.; Woodmansee, D. H.; Rafiq, A.; Sumser, M. P.; et al. AzoCholine Enables Optical Control of Alpha 7 Nicotinic Acetylcholine Receptors in Neural Networks. *ACS Chem. Neurosci.* **2015**, *6*, 701−707.
(10) Broichhagen, J.; Jurastow, I.; Iwan, K.; Kummer, W.; Trauner, D. Optical Control of Acetylcholinesterase with a Tacrine Switch. *Angew. Chem., Int. Ed.* **2014**, *53*, 7657−7660.
(11) Rastogi, S. K.; Zhao, Z.; Barrett, S. L.; Shelton, S. D.; Zafferani, M.; Anderson, H. E.; Blumenthal, M. O.; Jones, L. R.; Wang, L.; Li, X.; et al. Photoresponsive Azo-Combretastatin A-4 Analogues. *Eur. J. Med. Chem.* **2018**, *143*, 1−7.
(12) Ferreira, R.; Nilsson, J. R.; Solano, C.; Andréasson, J.; Grøtli, M. Design, Synthesis and Inhibitory Activity of Photoswitchable RET Kinase Inhibitors. *Sci. Rep.* **2015**, *5*, 9769.
(13) Pittolo, S.; Gómez-Santacana, X.; Eckelt, K.; Rovira, X.; Dalton, J.; Goudet, C.; Pin, J.-P.; Llobet, A.; Giraldo, J.; Llebaria, A.; et al. An Allosteric Modulator to Control Endogenous G Protein-Coupled Receptors with Light. *Nat. Chem. Biol.* **2014**, *10*, 813−815.
(14) Cheng, B.; Trauner, D.; Shchepakin, D.; Kavanaugh, M. P. A Photoswitchable Inhibitor of a Glutamate Transporter. *ACS Chem. Neurosci.* **2017**, *8*, 1668−1672.
(15) Schoenberger, M.; Damijonaitis, A.; Zhang, Z.; Nagel, D.; Trauner, D. Development of a New Photochromic Ion Channel Blocker via Azologization of Fomocaine. *ACS Chem. Neurosci.* **2014**, *5*, 514−518.
(16) Broichhagen, J.; Johnston, N. R.; von Ohlen, Y.; Meyer-Berg, H.; Jones, B. J.; Bloom, S. R.; Rutter, G. A.; Trauner, D.; Hodson, D. J. Allosteric Optical Control of a Class B G-Protein-Coupled Receptor. *Angew. Chem., Int. Ed.* **2016**, *55*, 5865−5868.
(17) Frank, J. A.; Yushchenko, D.; Fine, N. H. F.; Duca, M.; Citir, M.; Broichhagen, J.; Hodson, D. J.; Schultz, C.; Trauner, D. Optical Control of GPR40 Signalling in Pancreatic *β*-Cells. *Chem. Sci.* **2017**, *8*, 7604−7610.
(18) Awale, M.; Jin, X.; Reymond, J.-L. Stereoselective Virtual Screening of the ZINC Database Using Atom Pair 3D-Fingerprints. *J. Cheminf.* **2015**, *7*, 3.
(19) Burley, S. K.; Berman, H. M.; Kleywegt, G. J.; Markley, J. L.; Nakamura, H.; Velankar, S. Protein Data Bank (PDB): The Single Global Macromolecular Structure Archive. In *Protein Crystallography: Methods and Protocols*; Wlodawer, A., Dauter, Z., Jaskolski, M., Eds.; Methods in Molecular Biology; Springer New York: New York, NY, 2017; pp 627−641.
(20) Law, V.; Knox, C.; Djoumbou, Y.; Jewison, T.; Guo, A. C.; Liu, Y.; Maciejewski, A.; Arndt, D.; Wilson, M.; Neveu, V.; et al. DrugBank 4.0: Shedding New Light on Drug Metabolism. *Nucleic Acids Res.* **2014**, *42*, D1091−D1097.
(21) Bento, A. P.; Gaulton, A.; Hersey, A.; Bellis, L. J.; Chambers, J.; Davies, M.; Krüger, F. A.; Light, Y.; Mak, L.; McGlinchey, S.; et al. The ChEMBL Bioactivity Database: An Update. *Nucleic Acids Res.* **2014**, *42*, D1083−D1090.
(22) Groom, C. R.; Bruno, I. J.; Lightfoot, M. P.; Ward, S. C. The Cambridge Structural Database. *Acta Crystallogr., Sect. B: Struct. Sci., Cryst. Eng. Mater.* **2016**, *72*, 171−179.
(23) Sadowski, J.; Gasteiger, J. From Atoms and Bonds to Three-Dimensional Atomic Coordinates: Automatic Model Builders. *Chem. Rev.* **1993**, *93*, 2567−2581.
(24) da Silva, S. L.; Burbach, J. P. H. The Nuclear Hormone-Receptor Family in the Brain: Classics and Orphans. *Trends Neurosci.* **1995**, *18*, 542−548.
(25) Liu, S.; Downes, M.; Evans, R. M. Metabolic Regulation by Nuclear Receptors. In *Innovative Medicine: Basic Research and*

DOI: 10.1021/acscentsci.8b00881
ACS Cent. Sci. 2019, 5, 607−618

Development; Nakao, K., Minato, N., Uemoto, S., Eds.; Springer: Tokyo, 2015.
(26) Ordóñez-Morán, P.; Muñoz, A. Nuclear Receptors: Genomic and Non-Genomic Effects Converge. *Cell Cycle* **2009**, *8*, 1675−1680.
(27) Unsworth, A. J.; Flora, G. D.; Gibbins, J. M. Non-Genomic Effects of Nuclear Receptors: Insights from the Anucleate Platelet. *Cardiovasc. Res.* **2018**, *114*, 645−655.
(28) Kagechika, H.; Himi, T.; Namikawa, K.; Kawachi, E.; Hashimoto, Y.; Shudo, K. Retinobenzoic Acids. 3. Structure-Activity Relationships of Retinoidal Azobenzene-4-Carboxylic Acids and Stilbene-4-Carboxylic Acids. *J. Med. Chem.* **1989**, *32*, 1098−1108.
(29) Frank, J. A.; Yushchenko, D. A.; Hodson, D. J.; Lipstein, N.; Nagpal, J.; Rutter, G. A.; Rhee, J.-S.; Gottschalk, A.; Brose, N.; Schultz, C.; et al. Photoswitchable Diacylglycerols Enable Optical Control of Protein Kinase C. *Nat. Chem. Biol.* **2016**, *12*, 755−762.
(30) Frank, J. A.; Moroni, M.; Moshourab, R.; Sumser, M.; Lewin, G. R.; Trauner, D. *Nat. Commun.* **2015**, *6*, 7118.
(31) Frank, J. A.; Franquelim, H. G.; Schwille, P.; Trauner, D. Optical Control of Lipid Rafts with Photoswitchable Ceramides. *J. Am. Chem. Soc.* **2016**, *138*, 12981−12986.
(32) Haeggström, J. Z. Leukotriene A4 Hydrolase/Aminopeptidase, the Gatekeeper of Chemotactic Leukotriene B4 Biosynthesis. *J. Biol. Chem.* **2004**, *279*, 50639−50642.
(33) Çalıskan, B.; Banoglu, E. Overview of Recent Drug Discovery Approaches for New Generation Leukotriene A4 Hydrolase Inhibitors. *Expert Opin. Drug Discovery* **2013**, *8*, 49−63.
(34) Thunnissen, M. M. G. M.; Andersson, B.; Samuelsson, B.; Wong, C.-H.; Haeggström, J. Z. Crystal Structures of Leukotriene A4 Hydrolase in Complex with Captopril and Two Competitive Tight-Binding Inhibitors. *FASEB J.* **2002**, *16*, 1648−1650.
(35) Siewertsen, R.; Neumann, H.; Buchheim-Stehn, B.; Herges, R.; Näther, C.; Renth, F.; Temps, F. Highly Efficient Reversible Z−E Photoisomerization of a Bridged Azobenzene with Visible Light through Resolved S1(Nπ*) Absorption Bands. *J. Am. Chem. Soc.* **2009**, *131*, 15594−15595.
(36) Nicholls, A.; McGaughey, G. B.; Sheridan, R. P.; Good, A. C.; Warren, G.; Mathieu, M.; Muchmore, S. W.; Brown, S. P.; Grant, J. A.; Haigh, J. A.; et al. Molecular Shape and Medicinal Chemistry: A Perspective. *J. Med. Chem.* **2010**, *53*, 3862−3886.

DOI: 10.1021/acscentsci.8b00881
ACS Cent. Sci. 2019, 5, 607−618